Rewriting the Climatology of the Tropical North Atlantic and Caribbean Sea Atmosphere

JASON P. DUNION

NOAA/AOML/Hurricane Research Division, Miami, Florida

(Manuscript received 2 November 2009, in final form 25 June 2010)

ABSTRACT

The Jordan mean tropical sounding has provided a benchmark reference for representing the climatology of the tropical North Atlantic and Caribbean Sea atmosphere for over 50 years. However, recent observations and studies have suggested that during the months of the North Atlantic hurricane season, this region of the world is affected by multiple air masses with very distinct thermodynamic and kinematic characteristics. This study examined ~6000 rawinsonde observations from the Caribbean Sea region taken during the core months (July–October) of the 1995–2002 hurricane seasons. It was found that single mean soundings created from this new dataset were very similar to C. L. Jordan's 1958 sounding work. However, recently developed multispectral satellite imagery that can track low- to midlevel dry air masses indicated that the 1995–2002 hurricane season dataset (and likely Jordan's dataset as well) was dominated by three distinct air masses: moist tropical (MT), Saharan air layer (SAL), and midlatitude dry air intrusions (MLDAIs). Findings suggest that each sounding is associated with unique thermodynamic, kinematic, stability, and mean sea level pressure characteristics and that none of these soundings is particularly well represented by a single mean sounding such as Jordan's. This work presents three new mean tropical soundings (MT, SAL, and MLDAI) for the tropical North Atlantic Ocean and Caribbean Sea region and includes information on their temporal variability, thermodynamics, winds, wind shear, stability, total precipitable water, and mean sea level pressure attributes. It is concluded that the new MT, SAL, and MLDAI soundings presented here provide a more robust depiction of the tropical North Atlantic and Caribbean Sea atmosphere during the Atlantic hurricane season and should replace the Jordan mean tropical sounding as the new benchmark soundings for this part of the world.

1. Introduction

The first atmospheric climatology for the tropical North Atlantic and Caribbean Sea (TNAC) region was presented by Jordan (1958) more than 50 years ago and has served as a benchmark reference since that time. Jordan included a mean core month (July–October) hurricane season sounding in his 10-yr (1946–55) climatology that has been used extensively as a reference for tropical soundings during the North Atlantic hurricane season (Frank 1977; Gray and Craig 1998; Uhlhorn et al. 2007; Bryan and Rotunno 2009; Parodi and Emanuel 2009; Houze 2010; Molinari and Vollaro 2010) and as an initial background state in model simulations (Brown and Bretherton 1995; Ooyama 2001; Khain et al. 2008; Hill and Lackmann 2009; Fovell et al. 2009; Moon and Nolan 2010; Gall and Frank 2010). Jordan (1958) mentioned that since the tropics generally exhibit small spatial and seasonal variability, mean atmospheric soundings taken over the summer months in these regions should be robust. However, Carlson and Prospero (1972), Prospero and Carlson (1972), and Karyampudi and Carlson (1988) discussed a phenomenon called the Saharan air layer (SAL) and showed that this elevated layer (~1500–5500 m) of extremely warm, dry air and strong midlevel (~2000–4500 m) easterly winds that forms over West Africa can overspread vast areas of the tropical North Atlantic during the summer months. More recently, Dunion and Velden (2004) showed that individual SAL outbreaks can cover areas of the North Atlantic the size of the 48 contiguous United States and migrate as far west as the western Caribbean Sea and Gulf of Mexico. Dunion and Velden (2004) hypothesized that the components of the SAL can contribute to an environment that is hostile to tropical cyclone formation and intensification. They also suggested that in light of their findings related to the SAL, the TNAC is likely characterized by a multiple distribution of distinct environmental moisture soundings [e.g., SAL and non-SAL (moist tropical)] that are not well represented by

Corresponding author address: Jason P. Dunion, NOAA/AOML/Hurricane Research Division, 4301 Rickenbacker Causeway, Miami, FL 33149.
E-mail: jason.dunion@noaa.gov

DOI: 10.1175/2010JCLI3496.1

a single climatological sounding such as Jordan's (1958). They indicated that Jordan may have been unaware that his mean tropical sounding likely contained a mixture of SAL and non-SAL soundings. This suggests that the Jordan mean sounding is substantially drier than the typical moist tropical sounding that exists in the tropical North Atlantic during this time of year.

Dunion and Marron (2008) investigated Dunion and Velden's (2004) hypotheses regarding the possible influence of the SAL on the Jordan mean tropical sounding. They examined over 750 Caribbean rawinsonde soundings from July to October 2002 and presented evidence that the TNAC actually contains a mixture of SAL (~29%) and non-SAL (i.e., moist tropical; ~71%) air masses during these months. Their examination of a portion of Jordan's original dataset showed that a distinct two-peak probability distribution function (PDF; SAL and non-SAL soundings) existed, suggesting that although Jordan was likely unaware of it, his dataset probably contained a mixture of SAL and moist tropical soundings. The current study greatly expands on Dunion and Marron's (2008) work and presents new hurricane season mean soundings for the TNAC that are based on 8 years (1995–2002) of Caribbean rawinsonde data (6000 soundings). Findings from this work also resulted in the identification of an additional air mass that can significantly impact the TNAC during the Atlantic hurricane season: midlatitude dry air intrusions (MLDAIs). Discussion of the set of three new mean soundings [moist tropical (MT), SAL, and MLDAIs] is presented in detail and includes discussion on aspects of the mean state and temporal variability of their thermodynamics, kinematics, and stability. These new soundings represent a new benchmark for the TNAC region and could have important implications related to our understanding of the climatology for this part of the world.

2. Data and methods

This study examined twice-daily (0000 and 1200 UTC) rawinsonde observations from four Caribbean stations—Owen Roberts Airport, Grand Cayman [World Meteorological Organization (WMO) index: 78384]; Miami, Florida (WMO index: 72202); San Juan, Puerto Rico (WMO index: 78526); and La Raizet, Guadeloupe (WMO index: 78897)—for the period 1995–2002 [descriptions of the rawinsonde systems used at these sites are available in Dunion and Marron (2008)]. Sounding data were obtained from the University of Wyoming's online rawinsonde archive (http://weather.uwyo.edu/upperair/sounding.html). Figure 1 shows the locations of these rawinsonde stations as well as the geographical center (weighted by the total number of July–October soundings at each of the four stations) of the observations in the 1995–2002 dataset

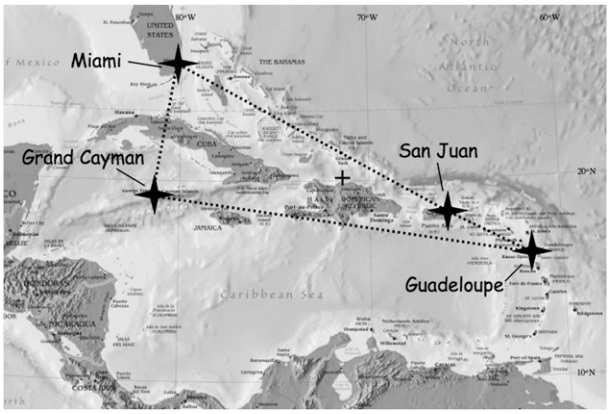

FIG. 1. Rawinsonde stations constituting the 1995–2002 rawinsonde dataset. The black cross located at 20.1°N, 71.3°W indicates the geographic center of the ~6000 rawinsondes observations used in the July–October 1995–2002 dataset (weighted by the number of soundings that were included from each of the four stations).

(20.1°N, 71.3°W). Geostationary Operational Environmental Satellite (GOES) multispectral infrared satellite imagery developed by Dunion and Velden (2004) [using techniques described by Dunion and Marron (2008)] was used to identify both moist (e.g., MT) and low- to midlevel dry air masses (e.g., the SAL and MLDAIs) that impacted each of the four rawinsonde sites at every rawinsonde launch time (0000 and 1200 UTC) over the 8-yr study period. The current work also employed the Hybrid Single-Particle Lagrangian Integrated Trajectory (HYSPLIT; Draxler and Rolph 2010) model running with National Centers for Environmental Prediction (NCEP)–National Center for Atmospheric Research (NCAR) reanalysis data to identify the origins of the air masses that were observed at these sites. Three-dimensional back trajectories were calculated to track the sources of low- to midlevel (850–700 hPa) moisture sampled by each of the rawinsondes in the dataset. Mosaics of total precipitable water from Remote Sensing Systems (RSS), GOES, and Meteosat visible satellite imagery and aerosol analyses from the Navy Aerosol Analysis and Prediction System (NAAPS; Zhang et al. 2008) were also used to examine the moisture and aerosol characteristics of the synoptic environments impacting the study region. Figure 2 shows a subset (1200 UTC 1, 10, 20, and 30 July–October 1995–2002) of 12-day HYSPLIT back trajectories (3000 m) originating from the four rawinsonde stations. These plots indicate that MT environments have a wide range of possible origins, while the SAL and MLDAI air masses have more distinct flow patterns across the North Atlantic. Although these trajectory plots only represent a portion (~350 trajectories) of the data used in this study, they are representative of the general air mass pathways found in the larger dataset.

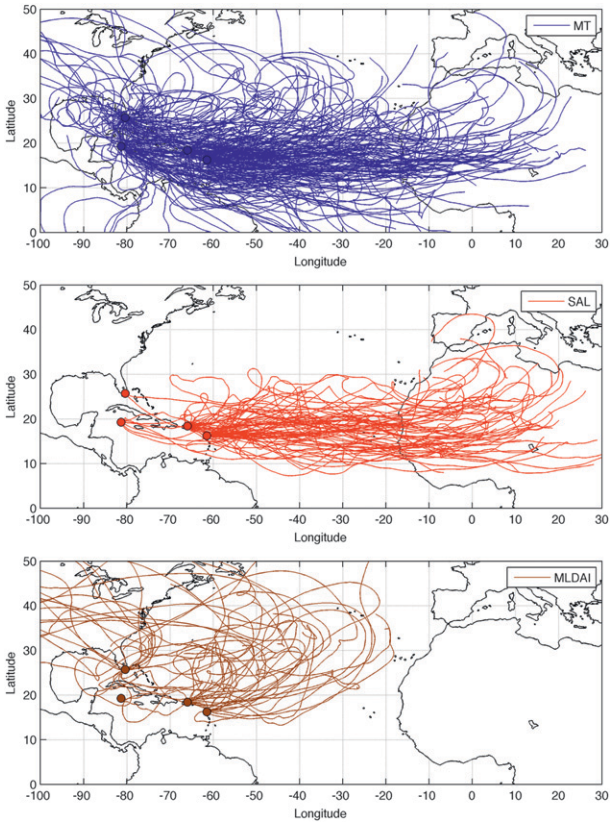

FIG. 2. Plots of HYSPLIT 12-day back trajectories (3000 m) originating from the four rawinsonde stations used in this study (Grand Cayman; Miami, FL; San Juan, PR; and La Raizet, Guadeloupe). Trajectories are shown for (top) MT, (middle) SAL, and (bottom) MLDAI air masses that were identified at 1200 UTC 1, 10, 20, and 30 July–October 1995–2002.

Approximately 7300 (6000) Caribbean rawinsonde observations for the months of June–October (July–October) were examined in this study. Rawinsondes from June were not included in the calculation of the new mean soundings. However, they were incorporated during the assessment of the seasonal variability of the three new sounding types. Mean (July–October) atmospheric soundings (presented at mandatory levels from the surface to 50 hPa),[1] stability indices, vertical wind shear, total precipitable water, and mean sea level pressure for three dominant air masses (MT, SAL, and MLDAI) that affect this region during the Atlantic hurricane season are presented. The mean July–October values of vertical wind shear and stability were derived from the ~6000 individual soundings (not from the single mean MT, SAL, and MLDAI soundings) in the 1995–2002 dataset. This methodology helped preserve the true wind vector and stability characteristics of the three sounding types, which would likely have been smoothed out in the averaging. Statistical significance among the mean values of the various thermodynamic, kinematic, and stability parameters for the three sounding types is presented. Significance was determined using a two-tailed Student's *t* test and, unless otherwise stated, these values are highly statistically significant at the 95%–99.9% level.

3. Results

a. 1995–2002 dataset versus Jordan (1958)

The July–October 1995–2002 dataset appears to be strikingly similar to Jordan's (1958) work. Figure 3 and Table 1 indicate that the average moisture sounding created from the ~6000 1995–2002 rawinsonde observations was quite similar (within 3.5% RH from the surface to 500 hPa) to Jordan's (1958) mean sounding.[2] Mixing ratio differences ranged from 0.1 to 0.3 g kg^{-1} from the surface to 500 hPa, and temperature disparities were less than 1.0°C from the surface to 100 hPa (2.5°C at 50 hPa). Geopotential height (GPH) differences were less than 7 m from the surface to 300 hPa and less than 25 m from 250 to 50 hPa. It should be noted that Jordan's mean hurricane season sounding did not include information on wind speed and direction. The thermodynamic and geopotential height differences between the two mean soundings suggest that the 1995–2002 and Jordan datasets are quite similar. This is comparable to results found by Dunion and Marron (2008). Although the mean 1995–2002 sounding was similar to Jordan's work and represents the average atmospheric conditions that exist during July–October in the TNAC, it does not appropriately represent the conditions that persist in this region at any particular time and place.

Analyses of the satellite, model, and rawinsonde data described in section 2 confirmed that three distinct air masses consistently affected the TNAC during the 1995–2002 hurricane seasons and that a single mean atmospheric sounding (like Jordan's) does not adequately represent this variability. Each of these air masses (MT,

[1] Mean thermodynamic, wind, and stability information for 600 hPa (not a mandatory level in routine sounding data) is also presented in this study. This was done because of the relatively large vertical gap (200 hPa) between the 500- and 700-hPa mandatory levels and was accomplished by extracting (from each individual sounding) the single level (if any existed) that was closest to (and within ±10 hPa of) 600 hPa. Although not as robust as the mandatory level data, these tight search constraints and large size of the sounding dataset (~6000 soundings) still produced statistically significant results.

[2] Humidity calculations in this study are presented in the WMO standard (with respect to water at all levels).

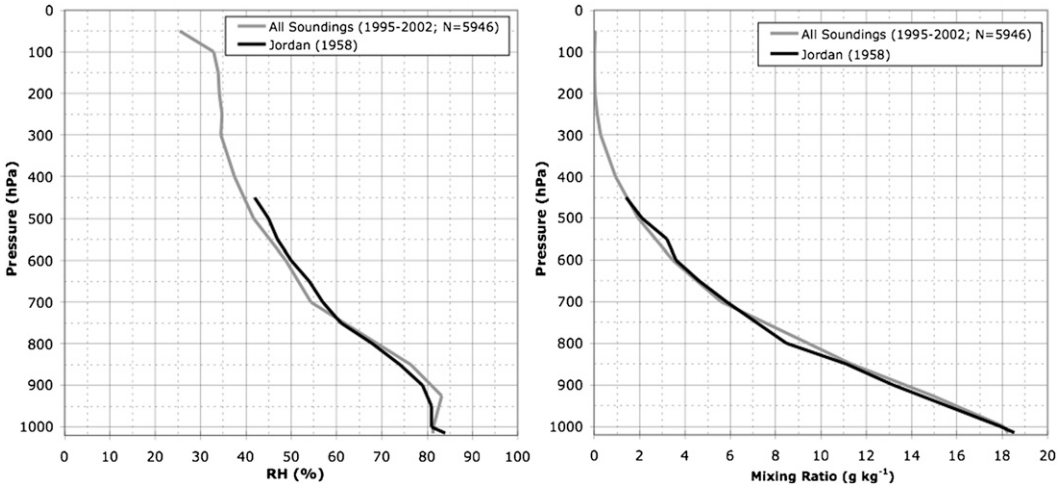

FIG. 3. Mean 1995–2002 (July–October) sounding vs the Jordan (1958) mean tropical sounding (July–October) for (left) RH (%) and (right) mixing ratio (g kg^{-1}).

SAL, and MLDAIs)[3] has very unique temporal variability, thermodynamic and kinematic profiles, stability characteristics, and vertical wind shear attributes. As discussed by Dunion and Marron (2008), it should be noted that the mean soundings presented in this study are more applicable to the tropical western and central North Atlantic and Caribbean Sea regions. The atmospheric and oceanic conditions found over the eastern North Atlantic are quite unique and mean soundings in this part of the basin would likely be different from those presented here (e.g., stronger temperature inversions at the SAL top and base, warmer temperatures in the SAL layer, stronger midlevel easterly jets, lower SAL bases and trade wind inversion levels, and cooler SSTs).

b. *Moist tropical, SAL, and midlatitude dry air intrusion soundings*

1) RELATIVE OCCURRENCE (INTRASEASONAL VARIABILITY)

GOES split-window satellite imagery (Dunion and Velden 2004; Dunion and Marron 2008), visible and microwave satellite imagery, and model analyses of parcel trajectories and atmospheric aerosols were used to identify various air masses that affected the Caribbean rawinsonde stations utilized in this July–October 1995–2002 study. Figure 4 shows the mean biweekly frequency distribution of MT, SAL, and MLDAI soundings for the period June–October (1995–2002) and indicates that the occurrence of each type of air mass varies significantly through the months of the hurricane season. The ~6000 July–October rawinsondes examined in this study reveal that, overall, the MT soundings account for ~⅔ (66%) of the soundings in the Caribbean. SAL outbreaks and MLDAIs account for 20% and 14% of the total soundings, respectively. Depending on the time of year, SAL frequency ranged from as much as ~40% (early summer) to as little as 2%–6% (October) of all soundings, while MLDAI frequency was consistently less than that of the SAL for all months except October. Though beyond the scope of this work, there are also interesting patterns in the spatial variability of the three sounding types [e.g., Grand Cayman (Guadeloupe) has the greatest percentage of MT (SAL) soundings, while Miami is impacted by the most MLDAIs]. These trends likely relate to the common flow patterns of the different air masses and the relative locations of the rawinsonde stations (Figs. 1 and 2).

Figure 4 indicates that the SAL is most active (large outbreaks that reach farther west) from mid-June to late July, when it constitutes ~40% of all Caribbean soundings. This confirms previous findings by Carlson and Prospero (1972) and Dunion and Marron (2008). Although SAL activity begins to gradually wane after July, SAL outbreaks can still impact the Caribbean through October. Not surprisingly, MLDAIs impact the Caribbean more rarely during the hurricane season and are most numerous in June and especially October when midlatitude frontal passages are relatively more common. Still, MLDAIs do consistently impact the tropical North Atlantic throughout

[3] Dunion and Marron (2008) also identified three unique air masses in their 2002 sounding study: non-SAL (moist tropical), SAL, and MLDAIs. Since MDLAIs made up a relatively small percentage (~10%) of their 2002 dataset, they decided to group these soundings together with the moist tropical soundings in their statistics. However, findings in the current study indicated that MLDAI soundings are actually more prevalent over the tropical North Atlantic Ocean. Therefore, this work presents three distinct soundings instead of just two.

TABLE 1. Jordan [1958 (italics)] and 1995–2002 [combined average (roman)] July–October mean atmospheric soundings from the current study.

Pressure (hPa)	GPH (m)	Temperature (°C)	Dewpoint (°C)	RH (%)	Mixing ratio (g kg^{-1})	Theta (K)	Theta-*e* (K)	Wind speed (m s^{-1})	Wind direction (°)
50	*20 743*	*−60.6*	—	—	—	*500.0*	—	—	—
	20 723	−63.1	−73.8	25.4	0.04	494.5	495.5	12.9	88
100	*16 568*	*−73.5*	—	—	—	*386.0*	—	—	—
	16 588	−74.4	−81.4	32.9	0.01	383.7	384.5	4.0	70
150	*14 177*	*−67.6*	—	—	—	*354.0*	—	—	—
	14 199	−67.0	−74.8	33.9	0.01	354.5	354.8	3.4	321
200	*12 396*	*−55.2*	—	—	—	*345.0*	—	—	—
	12 414	−54.4	−63.7	34.2	0.04	346.4	346.6	3.8	304
250	*10 935*	*−43.3*	—	—	—	*342.0*	—	—	—
	10 946	−42.6	−53.2	34.8	0.13	342.6	343.2	2.4	302
300	*9682*	*−33.2*	—	—	—	*338.0*	—	—	—
	9689	−32.6	−44.9	34.5	0.29	339.3	340.5	1.1	313
400	*7595*	*−17.7*	—	—	—	*332.0*	—	—	—
	7597	−17.3	−31.2	37.5	0.94	332.5	335.9	1.2	81
500	*5888*	*−6.9*	*−16.9*	*45.0*	*2.10*	*324.0*	*332.0*	—	—
	5888	−6.5	−20.4	41.7	1.94	325.0	331.8	2.3	93
600	*4442*	*1.4*	*−7.9*	*50.0*	*3.61*	*318.0*	*328.0*	—	—
	4439	1.7	−10.3	48.8	3.47	318.0	329.5	3.2	100
700	*3182*	*8.6*	*0.6*	*57.0*	*5.83*	*312.0*	*329.0*	—	—
	3180	9.1	−1.0	54.4	5.60	312.5	330.3	4.3	100
850	*1547*	*17.3*	*12.6*	*74.0*	*11.12*	*304.0*	*334.0*	—	—
	1543	17.4	12.9	76.4	11.34	304.4	338.5	5.3	101
925	—	—	—	—	—	—	—	—	—
	813	21.7	18.6	83.2	14.89	301.5	345.5	5.4	100
1000	*132*	*26.0*	*22.5*	*81.0*	*17.92*	*299.0*	*345.0*	—	—
	128	26.4	22.9	81.4	18.06	299.6	352.6	3.3	92
P_{MSL} = *1015.1*	—	*26.3*	*23.4*	*84.0*	*18.54*	*298.0*	*345.0*	—	—
P_{MSL} = 1015.3	—	26.9	23.3	81.3	18.26	298.9	352.3	2.0	91
Layer mean (850–500)	—	—	—	—	—	—	—	—	—
	—	6.7	−2.8	57.5	6.30	314.0	333.5	3.9	99

the hurricane season and appear to have sources that primarily originate from the North American continent, the central North Atlantic, and around the eastern side of the subtropical ridge (Fig. 2). HYSPLIT trajectory analyses indicate that this latter source of MLDAIs is often associated with significant subsidence. MLDAIs constitute over 35% of all Caribbean soundings in late October as midlatitude fronts begin to increasingly affect the subtropical and tropical North Atlantic and Caribbean. Interestingly, the number of October MLDAIs that impacted the Caribbean from 1995 to 2002 was significantly higher in El Niño years (1997 and 2002) than in non–El Niño years (1995–96 and 1998–2001; Bell and Halpert 1998, 2003). During the non–El Niño years, MLDAIs accounted for ~25% of all October soundings. However, in 2002 (a moderate El Niño year), 34% of the October soundings were MLDAIs (not shown), which is 1.5 standard deviations above the average for the non–El Niño years. In 1997 (the strongest El Niño on record; Bell and Halpert 1998), 47% of the October soundings were MLDAIs, which is more than 3.5 standard deviations above the average of the non–El Niño years. This suggests the possibility that during strong El Niño years, frontal activity in the tropical western North Atlantic and Caribbean is greatly enhanced in the late summer/early fall and the number of MLDAIs affecting this region increases significantly. Additionally, the following sections show that MLDAIs are associated with thermodynamic, stability, and especially vertical wind shear profiles that are hostile to tropical cyclone development. Although beyond the scope

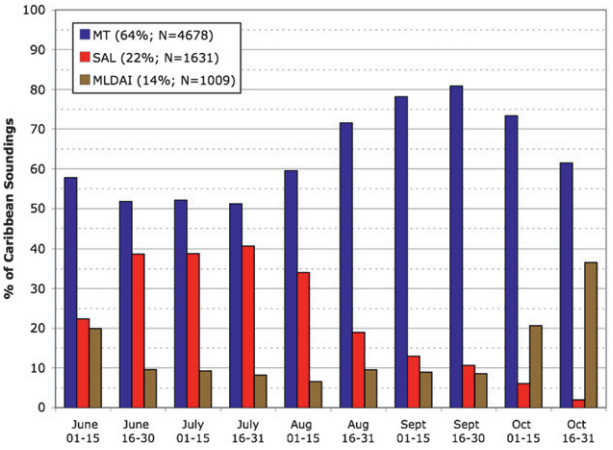

FIG. 4. Biweekly occurrences of MT, SAL, and MLDAI soundings from June to October (1995–2002) at the Grand Cayman, Miami, San Juan, and Guadeloupe rawinsonde stations. For the core months of the hurricane season (July–October) the occurrence of each sounding type (66% MT, $N = 3927$; 20% SAL, $N = 1212$; and 14% MLDAI, $N = 807$) was similar to the June–October period (see legend).

of this work, the possible connection between El Niño and increased occurrence of MLDAIs in the tropical western North Atlantic and Caribbean is an intriguing question and warrants further research.

MT environments constituted only 50%–60% of the Caribbean atmosphere from June through mid-August, but as SAL activity begins to subside in late July, the MT soundings gradually increase. By mid-August (and continuing through mid-October), MT soundings constitute 70%–80% of all Caribbean soundings. This agrees with previous work by DeMaria et al. (2001), who found that during the hurricane season, midlevel moisture in the tropical Atlantic reaches a minimum in mid-July and rapidly increases in mid-August. They surmised that this July moisture minimum might help explain why tropical cyclone genesis in the tropical Atlantic is relatively rare in July, even though vertical wind shear and instability typically become conducive for tropical cyclone development by the first week in July. Additionally, DeMaria and Kaplan (1994) defined a term called "relative intensity" that relates a tropical cyclone's maximum attained intensity to its maximum potential intensity (MPI). They found that for the months of the hurricane season, relative intensity was lowest in June and July, indicating that early-season storms are less likely to approach their MPI than mid- or late-season storms. This trend may partly relate to the fact that SAL activity peaks in these early summer months.

Interestingly, the mid-June to early August peak in SAL activity also corresponds quite well with the precipitation patterns described by Hastenrath (1967) and later termed the midsummer drought (MSD) by Magaña et al. (1999). Hastenrath (1967) described a pattern of abundant precipitation over Central America and the Caribbean during May and June, followed by an abrupt change around late June that ushered in a period of drier and less cloudy conditions in July and August. Though beyond the scope of this study, the midsummer peak in SAL activity may contribute to this relative minimum in the region's precipitation patterns and the onset of the midsummer drought.

Although MT soundings are the most prevalent of the three sounding types identified in this study, a significant portion of the core months of the hurricane season ($\sim 1/3$) is influenced by SAL or MLDAI environments. The following sections show that these two soundings are associated with thermodynamic, wind, and stability profiles that are not conducive to tropical cyclone development. This indicates that only $\sim 2/3$ of the time does the TNAC contain an environment (MT) that strongly supports tropical cyclone development and intensification.

2) MOISTURE

The mean MT, SAL, and MLDAI soundings that were extracted from the 1995–2002 rawinsonde dataset exhibited distinctly unique moisture characteristics. Although these three sounding types combine to create the "all soundings" moisture profiles shown in Fig. 3 and Table 1, none of them is particularly well represented by that single mean sounding or the Jordan (1958) mean sounding. Figure 5 shows that the MT sounding is significantly moister than the SAL and MLDAI soundings for every year in the 8-yr rawinsonde dataset, particularly in the lower to middle levels of the atmosphere. Figure 5 also indicates that the mean MT, SAL, and MLDAI soundings are fairly consistent from year to year. Figure 6 shows that at 700 hPa (the approximate vertical center of the SAL), the PDFs of the combined all sounding RH and mixing ratio are broad with multiple peaks. However, when the July–October (1995–2002) dataset is broken down by sounding type (MT, SAL, and MLDAI), the PDFs of moisture exhibit more distinct, single-peak tendencies. These results were also clearly evident at the 500- and 850-hPa levels (not shown). Figure 7 shows the statistical distributions of RH for the MT, SAL, and MLDAI soundings in the 1995–2002 Caribbean rawinsonde dataset using contoured frequency by altitude diagrams (CFADs). These CFADs highlight the differences between the three sounding types and their distinct distributions of vertical moisture. The RH CFADS have similarities to those presented by Brown and Zhang (1997), who looked at atmospheric moisture bimodality over the western Pacific Tropical Ocean and Global Atmosphere Coupled Ocean–Atmosphere Response Experiment (TOGA COARE) sounding network. Although the mean profiles

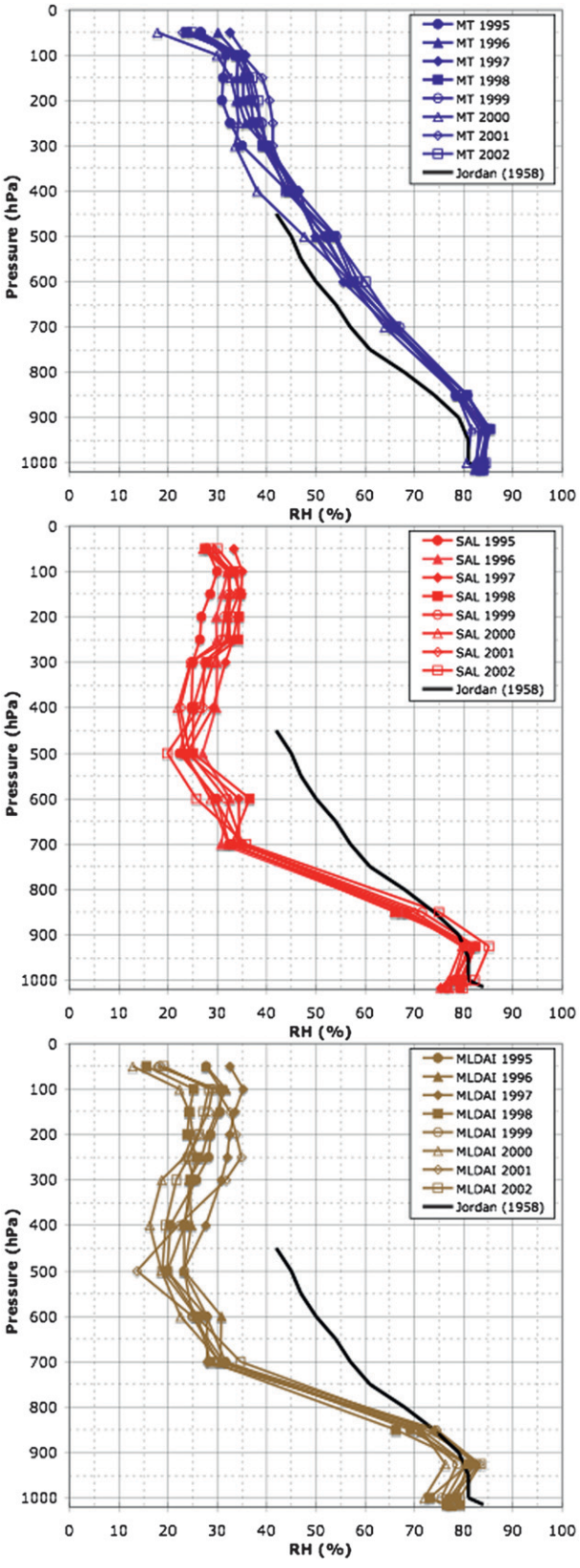

FIG. 5. Mean July–October soundings (for the years 1995–2002) of RH (%) for (top) MT, (middle) SAL, and (bottom) MLDAI air masses.

presented in the current work differ from those presented by Brown and Zhang (1997), clearly the presence of multiple sounding types is not unique to the North Atlantic.

Figure 8 and Table 2 show that the mean July–October (1995–2002) MT, SAL, and MLDAI moisture soundings are quite distinct (standard deviations of moisture for select pressure levels are listed in Table 3). The SAL and MLDAI soundings are 50%–60% (~30%–35% RH, 1.3–3.6 g kg^{-1}) drier than the MT sounding from 500 to 700 hPa and drier at every level below 50 hPa. Although the mean SAL and MLDAI moisture soundings are similar, the MLDAIs are drier than the SAL at every level from the surface to 150 hPa. These differences are most pronounced from the surface to 925 hPa, where the MLDAI mixing ratio is ~5%–10% (0.9–1.5 g kg^{-1}) drier than the SAL. This likely relates to the fact that unlike the SAL, MLDAIs are not purely elevated dry layers and are often associated with significant amounts of dry air in the boundary layer and surface layer. It is also worth noting that the RH differences between the SAL and MLDAI soundings are relatively small (<5% RH) from the surface to 925 hPa, even though the mixing ratio differences were relatively large (0.9–1.5 g kg^{-1}). This relates to the fact that MLDAIs are also associated with relatively cool low-level air that originates from midlatitudes, which acts to boost the RH (see next section). The moisture differences between the MT, SAL, and MLDAI soundings were highly statistically significant for all levels except 150 hPa (MT–SAL).

3) TEMPERATURE

Figure 6 indicates that the PDFs of the 700-hPa MT, SAL, and MLDAI temperatures exhibit distinct Gaussian distributions (confirmed by a chi-square goodness-of-fit test). The SAL distribution is shifted slightly to the right (relatively warmer temperatures) of the MT and MLDAI distributions, while the MLDAI distribution is broader and not as peaked as the MT and SAL distributions. Although the 700-hPa temperatures for the three sounding types are statistically unique, the differences are less striking than the moisture disparities. This was also found by Dunion and Marron (2008) and suggests that temperature is not as robust an indicator for identifying MT, SAL, and MLDAI soundings in the central and western tropical North Atlantic. Similar trends were also found at other pressure levels (not shown).

Figure 8 and Table 2 show that the mean July–October (1995–2002) MT, SAL, and MLDAI temperature soundings exhibit subtle differences (standard deviations of temperature for select pressure levels are listed in Table 3). Similar to findings by Dunion and Marron (2008), the SAL sounding is as much as 0.5°C warmer than the MT

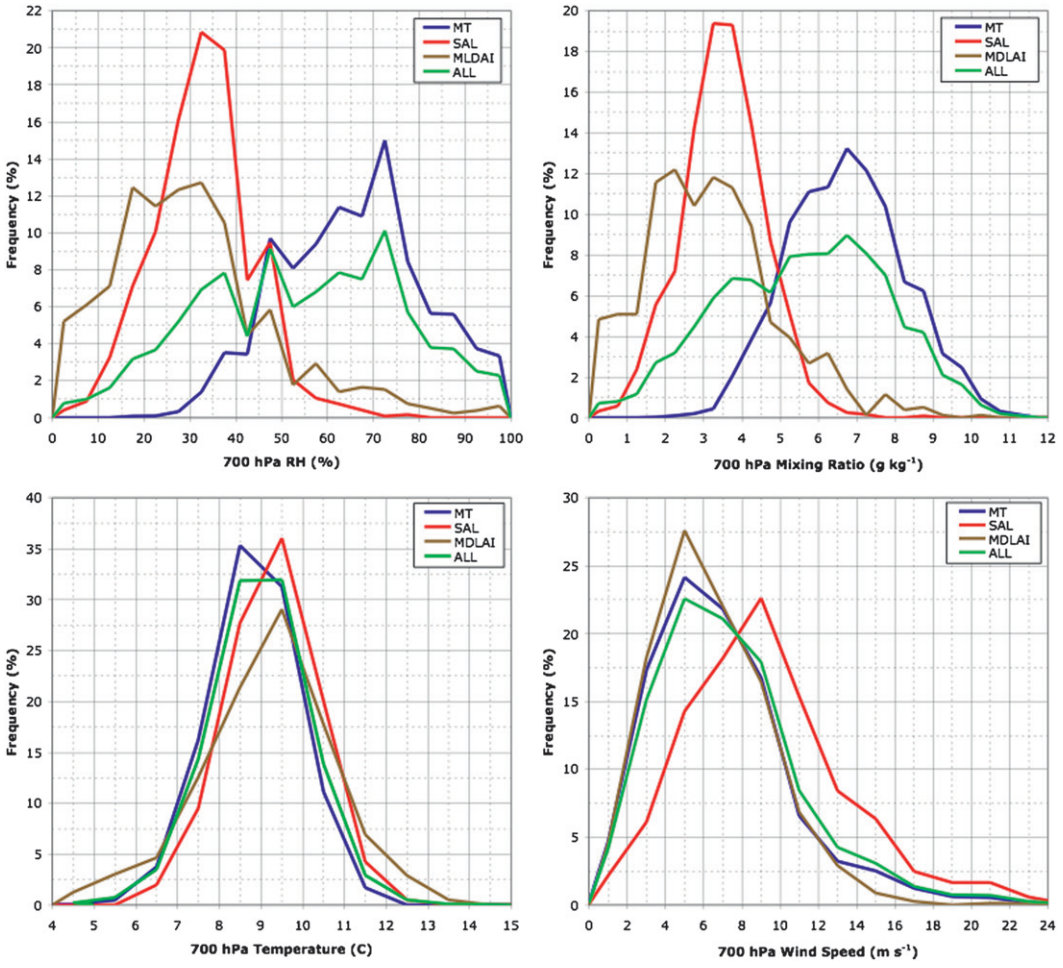

FIG. 6. PDFs of the rawinsondes that comprised the mean July–October (1995–2002) MT, SAL, and MLDAI 700-hPa soundings of (top left) RH (%), (top right) mixing ratio (g kg^{-1}), (bottom left) temperature (°C), and (bottom right) wind speed (m s^{-1}). The combined all-sounding 700-hPa PDFs of moisture, temperature, and wind speed are also included for reference.

sounding from 500 to 700 hPa, which relates to the SAL's origins over the hot Sahara Desert and to the fact that the SAL's warmth is partly preserved by solar heating of its suspended mineral dust (Carlson and Benjamin 1980; Dunion and Velden 2004; Dunion and Marron 2008). Surface temperatures in the SAL sounding were 0.8°C warmer than the MT sounding and may be due to the fact that the reduction in tropical convection associated with the relatively drier, more stable SAL environment is conducive to diminished cloud cover and increased overland surface heating.

Figure 8 and Table 2 also indicate that the MLDAI sounding is associated with the coolest lower-tropospheric temperatures and is related to the midlatitude origins of this air mass. These differences are most pronounced from the surface to 850 hPa, where the MLDAI sounding is 1.2°–1.3°C cooler than the MT and SAL soundings. The temperature differences between the MT, SAL, and MLDAI soundings were highly statistically significant for all levels except 50 hPa (MT–SAL), 250 hPa (SAL–MLDAI), and 500 hPa (SAL–MLDAI).

4) WINDS AND VERTICAL WIND SHEAR

Figure 6 shows that the PDFs of the 700-hPa MT, SAL, and MLDAI wind speeds exhibit lognormal distributions (confirmed by a chi-square goodness-of-fit test). The SAL distribution is shifted markedly to the right (relatively stronger midlevel winds) of the MT and MLDAI distributions and likely relates to the SAL's associated midlevel easterly jet. Although the MLDAI distribution indicates that midlevel winds in these air masses are similar to those of the MT environment, they tended to be the weakest of the three sounding types.

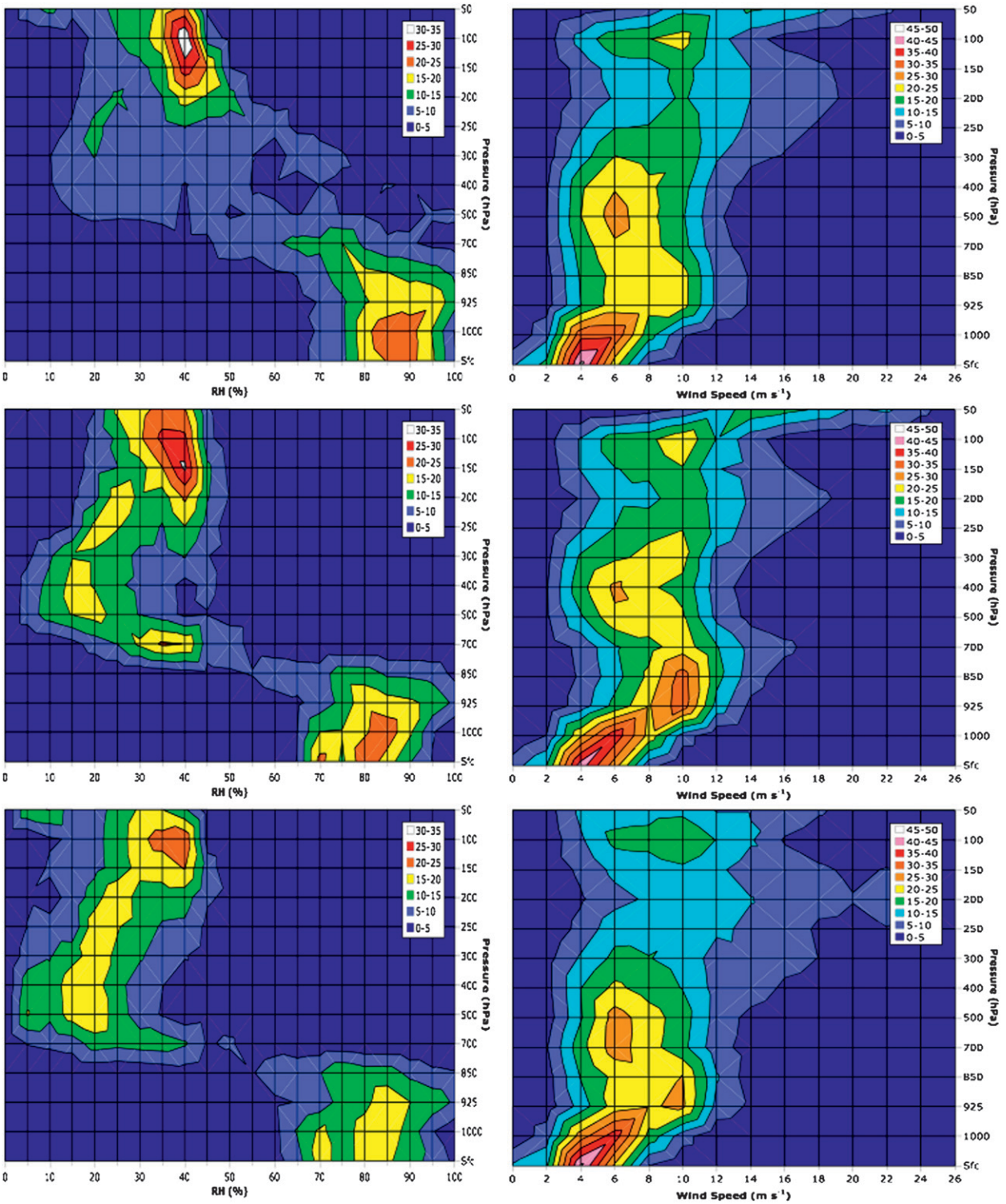

FIG. 7. Contoured frequency by altitude diagrams (CFADs) of (top) MT, (middle) SAL, and (bottom) MLDAI soundings as calculated from the July–October (1995–2002) Caribbean rawinsonde dataset. Contours represent the frequency of occurrence (see legend) of (left) RH (%) and (right) wind speed (m s^{-1}) at each level using bin sizes of 5% RH and 2 m s^{-1}, respectively.

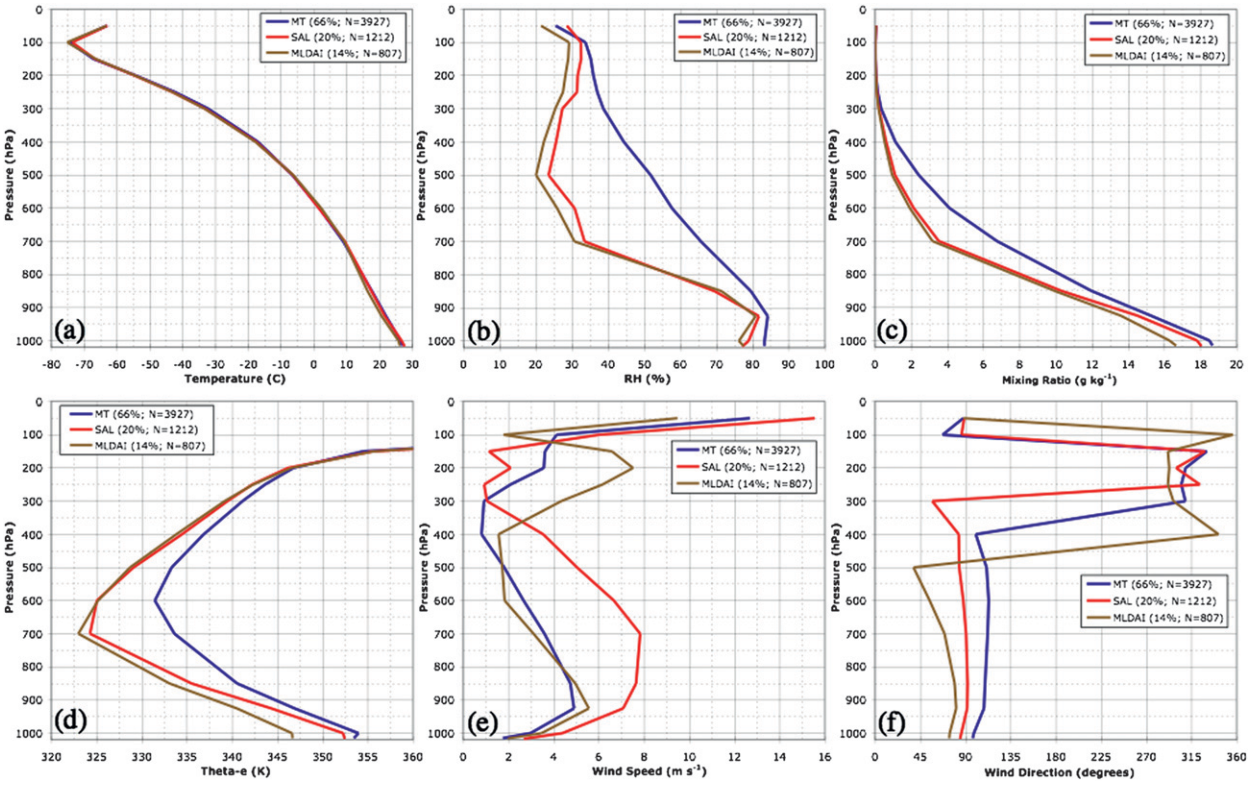

FIG. 8. Mean July–October (1995–2002) MT, SAL, and MLDAI soundings of (a) temperature (°C), (b) RH (%), (c) mixing ratio (g kg^{-1}), (d) theta-*e* (K), (e) wind speed (m s^{-1}), and (f) wind direction (°).

Figures 7 and 8 and Table 2 indicate that the wind profiles and vertical distributions of wind speed are quite different for the three sounding types (standard deviations of wind speed for select pressure levels are listed in Table 3). The MT sounding is associated with a deep layer (surface to 400 hPa) of light (~1–5 m s^{-1}) easterly trade winds overlaid by weak (~1–3.5 m s^{-1}) northwest winds from 300 to 150 hPa. Consequently, the 850–250-hPa vertical wind shear in the MT sounding is a moderate 8.2 m s^{-1} at 298° (Table 4).

In contrast to the MT sounding, the mean SAL sounding is associated with a slightly deeper layer (surface to 300 hPa) of easterly trades (Fig. 8 and Table 2). The SAL's low- to midlevel (850–500 hPa) winds were ~2–3 times stronger and more easterly than the MT sounding. These enhanced easterly winds are associated with the SAL's midlevel easterly jet and were also discussed in Dunion and Marron's (2008) study. Although the winds overlaying this trade wind profile are slightly shallower (250–150 hPa) than in the MT sounding, they are similarly weak (~1–2 m s^{-1}) and from the northwest. The 850–200-hPa vertical wind shear in the SAL sounding is a moderate to high 9.7 m s^{-1} and is primarily being driven by the SAL's midlevel easterly jet (Table 4). It should be noted that although the 850–200-hPa shear direction for the SAL sounding (278°) indicates westerly shear, it is actually the strong 850-hPa easterlies that are dominating the direction of this shear vector. Also, unlike the MT tropical sounding, the magnitude of the 700–200-hPa vertical wind shear in the SAL is nearly identical to the 850–200-hPa wind shear (Table 4). This is likely related to the deep easterly wind surge that is associated with the SAL.

The MLDAI sounding exhibits a relatively shallow layer (surface to 500 hPa) of light (~2–5.5 m s^{-1}) northeast to east-northeast winds under a deep layer (400–100 hPa) of northwest winds (Fig. 8 and Table 2). Above 300 hPa, these northwesterly winds are quite strong and peak at 200 hPa (7.5 m s^{-1}). This 200-hPa maximum is likely related to the fact that MLDAIs are often associated with midlatitude troughs and the upper-level jets that accompany these troughs. Although the low-level winds in the MLDAIs are fairly weak, the deep layer of relatively strong northwest winds in this profile results in a high value of mean 850–200-hPa vertical wind shear (12 m s^{-1}; Table 4). The 850–200-hPa shear direction for the MLDAI sounding is also westerly (280°), but in contrast to the SAL sounding, the MLDAI shear vector is being driven by strong 200-hPa winds. The wind speed differences between the MT, SAL, and MLDAI soundings were highly statistically

TABLE 2. MT (roman), SAL (boldface), and MLDAI (italics) July–October (1995–2002) mean atmospheric soundings.

Pressure (hPa)	GPH (m)	Temperature (°C)	Dewpoint (°C)	RH (%)	Mixing ratio (g kg^{-1})	Theta (K)	Theta-*e* (K)	Wind speed (m s^{-1})	Wind direction (°)
50	20 726	−63.0	−73.8	25.5	0.04	494.5	495.4	12.7	88
	20 733	**−63.0**	**−72.2**	**28.6**	**0.05**	**494.6**	**496.4**	**15.6**	**89**
	20 696	*−63.2*	*−75.4*	*21.5*	*0.04*	*494.1*	*495.1*	*9.5*	*88*
100	16 590	−74.5	−81.3	33.8	0.01	383.5	384.4	4.1	67
	16 593	**−73.7**	**−80.4**	**32.5**	**0.01**	**385.0**	**386.7**	**6.0**	**86**
	16 572	*−75.2*	*−83.1*	*29.2*	*0.004*	*382.2*	*382.8*	*1.8*	*356*
150	14 203	−67.2	−74.7	35.3	0.01	354.2	354.5	3.6	330
	14 196	**−66.8**	**−74.5**	**32.6**	**0.01**	**354.8**	**355.5**	**1.1**	**329**
	14 182	*−66.6*	*−75.6*	*29.0*	*0.01*	*355.2*	*355.6*	*6.6*	*292*
200	12 418	−54.3	−63.2	35.9	0.04	346.6	346.8	3.6	309
	12 413	**−54.7**	**−64.2**	**31.6**	**0.04**	**346.0**	**346.2**	**2.1**	**300**
	12 395	*−54.5*	*−65.3*	*28.2*	*0.03*	*346.3*	*346.5*	*7.5*	*293*
250	10 949	−42.3	−52.4	37.0	0.14	343.0	343.6	2.1	305
	10 947	**−43.1**	**−54.2**	**31.4**	**0.11**	**341.9**	**342.2**	**0.9**	**323**
	10 930	*−43.1*	*−55.9*	*27.6*	*0.09*	*341.9*	*342.3*	*6.2*	*292*
300	9690	−32.3	−43.5	38.7	0.34	339.8	341.1	0.9	309
	9693	**−33.1**	**−47.4**	**27.3**	**0.21**	**338.6**	**339.5**	**1.1**	**57**
	9676	*−33.3*	*−48.5*	*25.4*	*0.20*	*338.3*	*339.2*	*4.3*	*297*
400	7596	−17.1	−28.7	44.4	1.12	332.7	336.8	0.8	100
	7604	**−17.5**	**−35.1**	**25.7**	**0.61**	**332.1**	**334.4**	**3.5**	**83**
	7590	*−17.8*	*−37.2*	*22.2*	*0.52*	*331.8*	*333.8*	*1.6*	*342*
500	5887	−6.6	−16.9	51.8	2.41	325.0	333.3	1.8	111
	5897	**−6.4**	**−26.4**	**23.5**	**1.09**	**325.1**	**329.1**	**5.0**	**84**
	5883	*−6.3*	*−28.5*	*20.1*	*0.95*	*325.3*	*328.7*	*1.7*	*38*
600	4437	1.6	−7.1	57.7	4.11	317.9	331.4	2.7	113
	4451	**1.5**	**−16.5**	**30.7**	**2.13**	**317.8**	**325.0**	**6.7**	**88**
	4430	*2.2*	*−18.9*	*25.9*	*1.92*	*318.6*	*325.2*	*1.8*	*54*
700	3178	8.9	2.5	65.7	6.74	312.3	333.6	3.6	112
	3190	**9.4**	**−6.6**	**33.5**	**3.51**	**312.8**	**324.3**	**7.8**	**91**
	3173	*9.2*	*−9.5*	*30.7*	*3.17*	*312.7*	*323.0*	*3.1*	*69*
850	1541	17.6	13.8	79.5	11.96	304.6	340.5	4.7	109
	1553	**17.5**	**11.3**	**69.5**	**10.28**	**304.5**	**335.5**	**7.6**	**92**
	1542	*16.4*	*10.6*	*71.4*	*9.92*	303.3	333.1	*5.0*	*79*
925	810	21.9	19.0	84.2	15.27	301.7	346.9	4.9	108
	823	**21.6**	**18.2**	**81.7**	**14.53**	**301.4**	**344.3**	**7.1**	**92**
	815	*20.6*	*17.1*	*80.8*	*13.60*	*300.4*	*340.5*	*5.6*	*81*
1000	124	26.5	23.3	83.3	18.50	299.6	354.0	3.0	98
	138	**26.7**	**22.7**	**78.9**	**17.81**	**299.9**	**352.3**	**4.4**	**86**
	133	*25.8*	*21.1*	*76.2*	*16.28*	*298.9*	*346.6*	*3.5*	*74*
P_{MSL} = 1014.8	—	26.8	23.7	83.3	18.65	298.8	353.5	1.8	97
P_{MSL} = 1016.5	—	**27.6**	**23.2**	**77.2**	**18.04**	**299.5**	**352.5**	**2.7**	**84**
P_{MSL} = 1015.7	—	*26.2*	*21.8*	*77.6*	*16.65*	*298.1*	*346.7*	*2.0*	*74*
Layer mean (850–500)	—	6.7	−0.2	65.7	7.04	314.0	335.8	3.4	111
	—	**6.8**	**−7.2**	**42.2**	**4.97**	**314.1**	**329.6**	**6.8**	**89**
	—	*6.4*	*−9.0*	*40.9*	*4.70*	*313.7*	*328.3*	*3.2*	*69*

TABLE 3. Standard deviations of the MT, SAL, MLDAI, and combined average (i.e., all soundings) July–October (1995–2002) mean atmospheric soundings for select levels from 1000 to 200 hPa.

Pressure (hPa)	Sounding	GPH (m)	Temperature (°C)	RH (%)	Mixing ratio (g kg^{-1})	Wind speed (m s^{-1})
200	MT	41	1.6	14.2	0.02	7.0
	SAL	34	1.3	10.7	0.01	5.8
	MLDAI	56	1.6	13.0	0.02	9.7
	Combined average	43	1.6	13.9	0.02	7.4
500	MT	22	1.2	26.8	1.25	3.5
	SAL	18	1.3	16.2	0.71	3.1
	MLDAI	26	1.7	15.5	0.69	3.8
	Combined average	22	1.3	27.5	1.28	3.5
700	MT	22	1.1	15.7	1.50	3.9
	SAL	19	1.1	10.6	1.07	4.3
	MLDAI	19	1.6	18.1	1.73	3.2
	Combined average	22	1.2	21.9	2.16	4.0
850	MT	23	0.9	12.3	1.69	3.8
	SAL	17	1.2	17.8	2.34	3.0
	MLDAI	19	1.8	17.2	2.43	3.0
	Combined average	22	1.2	15.0	2.14	3.6
1000	MT	23	1.3	8.0	1.75	2.2
	SAL	18	0.9	7.8	1.88	2.1
	MLDAI	22	1.8	10.5	2.76	2.1
	Combined average	23	1.3	8.7	2.08	2.2

significant at all levels except 300 hPa (MT–SAL) and 500 hPa (MT–MLDAI).

5) STABILITY AND TPW

The MT, SAL, and MLDAI soundings exhibited distinct differences in stability [highly statistically significant for all parameters except level of free convection (SAL–MLDAI)] and total precipitable water (TPW) and are discussed in detail in this section. Low-level mixing is assumed in the calculations of lifted condensation level, level of free convection, convective available potential energy, convective inhibition, and lifted index and, therefore, the surface parcel is represented by the mean temperature and moisture in the lowest 500 m of each sounding. Additionally, pseudoadiabatic processes are assumed as the parcel is lifted.

(i) Lifted condensation level

The lifted condensation level (LCL) is defined as the height at which an air parcel being lifted dry adiabatically will become saturated because of adiabatic cooling and approximates the height of cloud base when there is mechanical forcing. Table 5 indicates that the MT sounding exhibits the lowest LCL (944 hPa) of the three soundings presented here, the result of its relatively high moisture content from the surface to 850 hPa. The SAL and MLDAI soundings exhibit relatively elevated LCL values (935 and 928 hPa, respectively), which relates to the drier lower-tropospheric air present in these soundings. The LCL values for these two soundings indicate that it is more difficult to form clouds in these environments (i.e., parcels must be lifted higher in the atmosphere to form clouds).

(ii) Level of free convection

The level of free convection (LFC) is the height at which a parcel of air—lifted dry adiabatically until it is saturated and lifted moist adiabatically thereafter—would first become warmer than the surrounding environment. The LFC also represents the point where the air parcel becomes positively buoyant and accelerates upward without further need for forced lifting. If more than one LFC existed in a sounding, the lowest level was chosen. Also, if the parcel was positively buoyant throughout the sounding, the LFC was set to be the same as the LCL. Table 5 indicates that the MT sounding has the lowest LFC (880 hPa)

TABLE 4. 700–200-hPa and 850–200-hPa vertical wind shear for the MT, SAL, MLDAI, and combined average (i.e., all soundings) July–October (1995–2002) mean atmospheric soundings. Both the shear magnitude and direction are shown.

Layer (hPa)	Sounding	Speed (m s^{-1})	Direction (°)
700–200	MT	7.1	300
	SAL	9.8	277
	MLDAI	10.0	281
	Combined average	7.9	291
850–200	MT	8.2	298
	SAL	9.7	278
	MLDAI	12.0	280
	Combined average	8.9	290

TABLE 5. Stability and moisture indices from the MT, SAL, MLDAI, and combined average (i.e., all soundings) July–October (1995–2002) mean atmospheric soundings.

	LCL (hPa)	LFC (hPa)	CAPE (J kg^{-1})	CIN (J kg^{-1})	KI	LI	TPW (mm)
MT	944.0	879.5	1922	−22.9	31.5	−4.4	51.5
SAL	935.3	862.8	1731	−32.8	19.2	−3.7	40.1
MLDAI	927.7	860.0	1046	−28.0	14.6	−1.6	37.6
Combined average	940.0	873.6	1765	−25.7	26.7	−3.9	47.3

of the three soundings. The LFC in the SAL sounding is ~17 hPa higher (863 hPa) than the MT sounding and relates to the SAL's dry lower-tropospheric air and low- to midlevel warmth. The MLDAI sounding has the highest LFC (860 hPa; ~20 hPa higher than the MT sounding), which relates to its dry lower-tropospheric air and relatively cooler surface temperatures.

(iii) Convective available potential energy

Convective available potential energy (CAPE) is defined as the amount of energy a parcel of air would have if lifted a certain distance vertically through the atmosphere. The CAPE calculations used in this study did not include virtual temperature effects and entrainment was neglected. Table 5 shows that the CAPE in the MT sounding is 1922 J kg^{-1}, indicating a moderately unstable environment. The CAPE in the SAL sounding is ~10% less (1731 J kg^{-1}) and also indicates a moderately unstable environment. However, there are several competing effects present in the SAL soundings that combine to produce a net reduction in CAPE (relative to the MT sounding): 1) the SAL is warmer from the surface to 1000 hPa, which would help boost CAPE; 2) the SAL's LCL is higher, so a parcel will be relatively cooler when lifted to its LFC (less CAPE); 3) the SAL's LFC is higher, which would equate to potentially less CAPE; 4) the SAL's low- to midlevel warmth would tend to reduce CAPE; and 5) SAL soundings are associated with a dry middle layer aloft that is often closer to dry adiabatic, which would boost CAPE. Although these various competing effects result in a SAL sounding that has relatively less CAPE, the details are certainly more complex. Another important consideration is that the CAPE calculations neglected entrainment effects. It is likely that the low- to midlevel moisture differences between the MT, SAL, and MLDAI soundings would result in relatively reduced buoyancy in the SAL and MLDAIs (this reduced buoyancy would not be fully captured by a standard CAPE calculation).

The CAPE in the MLDAI sounding is only 1046 J kg^{-1}, indicating an only marginally to moderately unstable profile. This relatively low CAPE likely relates to the fact that this sounding is associated with the highest LCL and LFC and is substantially drier than the MT sounding and somewhat drier than the SAL sounding.

(iv) Convective inhibition

Convective inhibition (CIN) is a measure of the amount of energy needed to lift an air parcel from the surface to the LFC and can be quite pronounced when a layer of relatively warm air is located above the surface layer (i.e., a temperature inversion exists). Table 5 shows that CIN is smallest (least negative) in the MT sounding (−22.9 J kg^{-1}), indicating a fairly unstable environment. Since the SAL is associated with warm temperatures in the lower to middle levels (~850–500 hPa) and typically has a strong temperature inversion at its base, it is not surprising that CIN values for this sounding are the largest (−32.8 J kg^{-1}). Since the mean height of the LFC is 863 hPa in the SAL and the low-level temperature inversion at the SAL's base is typically found above that level (~850–800 hPa), CIN is probably only capturing the stabilizing effects of the SAL's low-level temperature inversion and warmth a portion of the time. The CIN for the MLDAI sounding (−28.0 J kg^{-1}) was 5.1 J kg^{-1} larger than for the MT sounding and is in part related to the fact that this sounding has the most elevated LFC (860 hPa). Additionally, the extreme lower-tropospheric dryness of the MLDAI sounding would promote nighttime radiational cooling and help to enhance the formation of low-level nocturnal temperature inversions, which would also act to enhance CIN.

(v) K index

The *K* index (KI) is a measure of the thunderstorm potential based on the vertical temperature lapse rate, moisture content of the lower troposphere, and the vertical extent of the moist layer (George 1960). Table 5 shows that the KI for the MT sounding is 31.5, indicating an environment that is conducive for scattered thunderstorm activity. The extreme low- to midlevel dryness in the SAL and MLDAI soundings (and midlevel warmth of the SAL sounding) equate to much lower KI values of 19.2 and 14.6, respectively. It should be noted that KI values of less than 20 suggest an environment with little to no thunderstorm activity.

(vi) Lifted index

The lifted index (LI) is calculated by taking a representative low-level air parcel and lifting it adiabatically to

TABLE 6. Percentage of moisture below a given pressure level for the MT, SAL, MDLAI, and combined average (i.e., all soundings) July–October (1995–2002) mean atmospheric soundings. Percentages were weighted according to the thickness of each layer.

Pressure (hPa)	MT	SAL	MLDAI	All soundings
50	99.996	99.994	99.996	99.996
100	99.9	99.8	99.9	99.9
150	99.8	99.8	99.8	99.8
200	99.8	99.7	99.7	99.7
250	99.6	99.5	99.5	99.6
300	99.1	99.0	99.1	99.1
400	96.5	97.2	97.3	96.7
500	91.2	94.0	94.4	92.2
600	83.0	88.7	89.3	84.7
700	71.1	80.6	81.4	73.7
850	43.8	55.1	54.3	46.6
925	26.3	33.0	32.9	28.1
1000	4.7	6.0	5.9	5.1

500 hPa. The temperature difference between this air parcel and the ambient environment at 500 hPa denotes the LI. Table 5 shows that the LI for the MT sounding is −4.4, indicating an unstable environment with thunderstorm development likely. The LI for the SAL sounding is slightly more stable (−3.7) and is also indicative of an unstable environment with thunderstorm development likely. Since LI utilizes the LCL in its calculation, it does inherently account for low-level moisture but does not adequately account for midlevel dryness. Therefore, since the SAL is only slightly drier than the MT sounding below ~850 hPa and its LCL is only ~9 hPa higher, LI differences between the two soundings are not exceptionally large. The LI for the MLDAI sounding is −1.6, indicating a marginally unstable atmosphere with thunderstorms possible. This sounding is ~1.0°–1.5°C cooler and ~1.0–2.0 g kg^{-1} drier than the MT and SAL soundings from the surface to 850 hPa and likely why its LI is significantly more stable than the MT and SAL soundings.

(vii) TPW

TPW is a measurement of the amount of water vapor in a column extending from the surface to the top of the atmosphere. This quantity can be reliably derived from satellites using the 19-, 22-, and 37-GHz microwave channels [e.g., from the Special Sensor Microwave Imager (SSM/I)] and is one of the most accurate and robust of the microwave-derived satellite products (Alishouse et al. 1990; Ferraro et al. 1996). One significant advantage of microwave-derived TPW over the GOES split-window algorithm developed by Dunion and Velden (2004) is that it can detect atmospheric moisture through clouds. Therefore, it is an ideal tool for tracking air masses such as MT, SAL, and MLDAIs. Table 6 indicates that ~90%–95% of the total column moisture is below 500 hPa in all three sounding types. Since such a large percentage of the column moisture is contained in the lower to middle levels (surface to 500 hPa) of the atmosphere, TPW is an extremely robust proxy for detecting dry air masses like the SAL and MLDAIs. In fact, moisture variability in these parts of the vertical column can result in large differences in TPW. Table 5 shows that the TPW in the MT sounding is 51.5 mm, indicating a relatively moist low- to midlevel environment. The SAL sounding contains ~20% less TPW (~40 mm) than the MT sounding, while the MLDAI sounding contains ~25%–30% less moisture (~37.5 mm) than the MT sounding. The SAL's 850–500-hPa dryness is responsible for the low TPW values in the SAL sounding, while the even lower TPW in the MLDAI sounding is being driven by both its midlevel dryness and its relatively drier air from the surface to 850 hPa. The means and standard deviations of TPW for these three air masses (not shown) suggest that 45 mm is a reasonable threshold value for discerning MT air masses from environments with substantially dry air in the lower to middle levels (e.g., SAL and MLDAI air masses).

6) GEOPOTENTIAL HEIGHT AND MEAN SEA LEVEL PRESSURE

Table 1 indicates that the mean sea level pressure P_{MSL} for the TNAC is 1015.3 hPa. However, significant surface pressure differences exist between the three sounding types that constitute this mean value. Table 2 indicates that below 250 hPa, the SAL sounding exhibited the highest geopotential heights of the three sounding types, while the MLDAI sounding had the lowest heights from 700 to 50 hPa. Not surprisingly, the SAL sounding was associated with the highest mean surface pressure (1016.5 hPa), while the MLDAI sounding had a relatively lower mean surface pressure (1015.7 hPa). The mean surface pressure was lowest for the MT sounding (1014.8 hPa), indicating that in terms of pressure, it is the most conducive environment for tropical cyclone development. The MT sounding had the lowest mean surface pressure for every month from June to October, while the SAL sounding exhibited the highest mean surface pressure for all months except October.

The relatively high surface pressure of the SAL sounding (1.7 and 0.8 hPa higher than the MT and MLDAI soundings, respectively) is related to the fact that it is typically positioned in the ridge that is located either in front of or, more typically, behind African easterly waves that propagate across the North Atlantic during the summer. Karyampudi and Carlson (1988) noted a "curious" clockwise rotation of the SAL in their three-dimensional conceptual model of the SAL, which is probably related to this ridge positioning. The SAL's higher pressure may equate to relatively stronger subsidence within this unique

environment and might help explain why the mean SAL sounding is so dry at levels well above its typical upper extent (~500 hPa). Since SAL outbreaks take several days to cross the basin, this subsidence-induced drying would be particularly evident in soundings taken well west of the SAL's source over Africa (i.e., the soundings used in this study). The MLDAI sounding's lower pressure (relative to the SAL) is likely related to the fact that these air masses are often associated with midlatitude troughs (i.e., relatively lower pressure). However, the relatively cooler temperatures of the MLDAI sounding may somewhat offset this lower pressure, producing slightly higher pressure compared to the MT sounding.

4. Concluding remarks

A new set of mean soundings representing the core months of the North Atlantic hurricane season (July–October) is presented for the tropical North Atlantic and Caribbean Sea region. This dataset includes ~6000 Caribbean rawinsonde observations for the 8-yr period 1995–2002 and was shown, in the mean, to be very similar to the sounding work presented by Jordan in 1958. However, GOES multispectral satellite imagery, three-dimensional HYSPLIT model trajectories, mosaics of total precipitable water, GOES and Meteosat visible satellite imagery, and aerosol analyses from the NAAPS model indicated that the 1995–2002 sounding dataset was dominated by three distinct air masses: moist tropical (MT; 66% of all soundings), Saharan air layer (SAL; 20% of all soundings), and midlatitude dry air intrusions (MLDAIs; 14% of all soundings). These three sounding types were each associated with distinct temporal (intraseasonal) variability, thermodynamics, kinematics, wind shear, stability attributes, and surface pressures; none is particularly well represented by a single climatological sounding such as Jordan's (1958). It is concluded that the new MT, SAL, and MLDAI soundings presented here provide a more robust depiction of the tropical North Atlantic and Caribbean Sea atmosphere during the Atlantic hurricane season and should replace the Jordan mean tropical sounding as the new benchmark soundings for this part of the world.

The new atmospheric sounding information presented here represents a new standard for the tropical North Atlantic and Caribbean Sea region and could have important implications related to our understanding of the climatology for this region of the globe. Additionally, this work could help enhance our understanding of intra- and interannual climate variability in the region and has relevance to tropical cyclone forecasting and modeling.

Acknowledgments. The author would like to thank the following students for their contributions to this study: Christopher Marron, Andrew Hagen, Dorianne Alvarado, Debbie Ruperto, Cristimer Gonzalez, and Juliana Gil. Special thanks also to Robert Burpee, John Kaplan, Gary Barnes, and Scott Braun for many insightful discussions throughout various stages of this research project. This paper benefited from reviews by John Kaplan and Stan Goldenberg of the NOAA/AOML/Hurricane Research Division, Mark DeMaria from NOAA/NESDIS, and two anonymous reviewers. Special thanks also to Paige for her many hours of help with this manuscript.

REFERENCES

Alishouse, J., S. Snyder, J. Vongsathorn, and R. Ferraro, 1990: Determination of oceanic total precipitable water from the SSM/I. *IEEE Trans. Geosci. Remote Sens.,* **28,** 811–816.

Bell, G. D., and M. S. Halpert, 1998: Climate Assessment for 1997. *Bull. Amer. Meteor. Soc.,* **79,** S1–S51.

——, and ——, 2003: ENSO and the tropical Pacific. *Bull. Amer. Meteor. Soc.,* **84,** S1–S68.

Brown, R. G., and C. S. Bretherton, 1995: Tropical wave instabilities: Convective interaction with dynamics using the Emanuel convective parameterization. *J. Atmos. Sci.,* **52,** 67–82.

——, and C. Zhang, 1997: Variability of midtropospheric moisture and its effect on cloud-top height distribution during TOGA COARE. *J. Atmos. Sci.,* **54,** 2760–2774.

Bryan, G. H., and R. Rotunno, 2009: The influence of near-surface, high-entropy air in hurricane eyes on maximum hurricane intensity. *J. Atmos. Sci.,* **66,** 148–158.

Carlson, T. N., and J. M. Prospero, 1972: The large-scale movement of Saharan air outbreaks over the northern equatorial Atlantic. *J. Appl. Meteor.,* **11,** 283–297.

——, and S. G. Benjamin, 1980: Radiative heating rates for Saharan dust. *J. Atmos. Sci.,* **37,** 193–213.

DeMaria, M., and J. Kaplan, 1994: Sea surface temperature and the maximum intensity of Atlantic tropical cyclones. *J. Climate,* **7,** 1324–1334.

——, J. A. Knaff, and B. H. Connell, 2001: A tropical cyclone genesis parameter for the tropical Atlantic. *Wea. Forecasting,* **16,** 219–233.

Draxler, R. R., and G. D. Rolph, cited 2010: HYSPLIT—Hybrid Single Particle Lagrangian Integrated Trajectory Model. [Available online at http://ready.arl.noaa.gov/HYSPLIT.php.]

Dunion, J. P., and C. S. Velden, 2004: The impact of the Saharan air layer on Atlantic tropical cyclone activity. *Bull. Amer. Meteor. Soc.,* **85,** 353–365.

——, and C. S. Marron, 2008: A reexamination of the Jordan mean tropical sounding based on awareness of the Saharan air layer: Results from 2002. *J. Climate,* **21,** 5242–5253.

Ferraro, R. R., N. C. Grody, F. Weng, and A. Basist, 1996: An eight-year (1987–1994) time series of rainfall, clouds, water vapor, snow cover, and sea ice derived from SSM/I measurements. *Bull. Amer. Meteor. Soc.,* **77,** 891–905.

Fovell, R. G., K. L. Corbosiero, and H. Kuo, 2009: Cloud microphysics impact on hurricane track as revealed in idealized experiments. *J. Atmos. Sci.,* **66,** 1764–1778.

Frank, W. M., 1977: The structure and energetics of the tropical cyclone I. Storm structure. *Mon. Wea. Rev.,* **105,** 1119–1135.

Gall, J. S., and W. M. Frank, 2010: The role of equatorial Rossby waves in tropical cyclogenesis. Part II: Idealized simulations

in a monsoon trough environment. *Mon. Wea. Rev.,* **138,** 1383–1398.

George, J. J., 1960: *Weather Forecasting for Aeronautics*. Academic Press, 673 pp.

Gray, S. L., and G. C. Craig, 1998: A simple theoretical model for the intensification of tropical cyclones and polar lows. *Quart. J. Roy. Meteor. Soc.,* **124,** 919–947.

Hastenrath, S., 1967: Rainfall distribution and regime in Central America. *Arch. Meteor. Geophys. Bioklimatol.,* **15B,** 201–241.

Hill, K. A., and G. M. Lackmann, 2009: Analysis of idealized tropical cyclone simulations using the weather research and forecasting model: Sensitivity to turbulence parameterization and grid spacing. *Mon. Wea. Rev.,* **137,** 745–765.

Houze, R. A., Jr., 2010: Clouds in tropical cyclones. *Mon. Wea. Rev.,* **138,** 293–344.

Jordan, C. L., 1958: Mean soundings for the West Indies area. *J. Meteor.,* **15,** 91–97.

Karyampudi, V. M., and T. N. Carlson, 1988: Analysis and numerical simulations of the Saharan air layer and its effect on easterly wave disturbances. *J. Atmos. Sci.,* **45,** 3102–3136.

Khain, A., N. Cohen, B. Lynn, and A. Pokrovsky, 2008: Possible aerosol effects on lightning activity and structure of hurricanes. *J. Atmos. Sci.,* **65,** 3652–3677.

Magaña, V., J. A. Amador, and S. Medina, 1999: The midsummer drought over Mexico and Central America. *J. Climate,* **12,** 1577–1588.

Molinari, J., and D. Vollaro, 2010: Distribution of helicity, CAPE, and shear in tropical cyclones. *J. Atmos. Sci.,* **67,** 274–284.

Moon, Y., and D. S. Nolan, 2010: Do gravity waves transport angular momentum away from tropical cyclones? *J. Atmos. Sci.,* **67,** 117–135.

Ooyama, K. V., 2001: A dynamic and thermodynamic foundation for modeling the moist atmosphere with parameterized microphysics. *J. Atmos. Sci.,* **58,** 2073–2102.

Parodi, A., and K. Emanuel, 2009: A theory for buoyancy and velocity scales in deep moist convection. *J. Atmos. Sci.,* **66,** 3449–3463.

Prospero, J. M., and T. N. Carlson, 1972: Vertical and areal distributions of Saharan dust over the western equatorial North Atlantic Ocean. *J. Geophys. Res.,* **77,** 5255–5265.

Uhlhorn, E. W., P. G. Black, J. L. Franklin, M. Goodberlet, J. Carswell, and A. S. Goldstein, 2007: Hurricane surface wind measurements from an operational stepped frequency microwave radiometer. *Mon. Wea. Rev.,* **135,** 3070–3085.

Zhang, J., J. S. Reid, D. L. Westphal, N. L. Baker, and E. J. Hyer, 2008: A system for operational aerosol optical depth data assimilation over global oceans. *J. Geophys. Res.,* **113,** D10208, doi:10.1029/2007JD009065.